Rocket Launch Noise at Santa Maria Spaceport

João Paulo Soares
joaopaulosoares@tecnico.ulisboa.pt

Instituto Superior Técnico, Universidade de Lisboa, Portugal

November 2021

Abstract

The rocket exhaust plume radiates intense acoustic levels which vibrate the launch related structures and affect a radius of kilometers, which can include communities near the launch site. As such understanding the vibroacoustics of the rocket during lift off has been an important subject to avoid damage to the vehicle, payload, ground systems, launch tower and nearby communities livelihood. The latter will be subject of this study, where the far-field rocket noise prediction methods are implemented through out the early stages of flight of the rocket. This work compares the methods and different models associated with them to experimental data and discusses their validity for a rocket in motion. With the numerical models established, noise contours and metrics were computed for nearby regions in the Santa Maria spaceport, considering the Electron and Falcon 9 rockets.

Keywords: launch noise, acoustics, trajectory, prediction, directivity.

1. Introduction

The Santa Maria spaceport is set to become an important project for the democratisation of space, as it entails the sustainable integration of space within society and economic development. This includes access to space data and to space itself [1].

This work will assess the impact in the island of Santa Maria of the noise from launching rockets launch at early stages of the trajectories, for the case of small to medium launchers. With the integration of a space launch facility near a populated area various concerns arise and the rockets launch noise is a subject to be tackled.

The complex behaviour of the exhaust flow at the nozzle exit showed the need to adapt the theoretical approach to fit the experimental data [2], this provided room for the emergence of empirical models of noise prediction. NASA set forth three semi-empirical models [3], where two have been the foundation for all subsequent models, the Distribution Source Method 1 (DSM-1) and Distribution Source Method 2 (DSM-2), even if they are not consistent with the generally accepted Lighthill's jet noise theory [4]. Experimental data over the years has improved and corrected the assumptions made in the Eldred model, and some suggested improvements will be discussed in this work.

2. Rocket Launch Noise Prediction

2.1. Empirical Model Formulation

The acoustic loads generated by the propulsion system of a space vehicle at launch is determined by semi-empirical methods due to the complex phenomena in the generation of sound in supersonic jets [2]. The noise prediction methodologies that are most often used are based on a source allocation technique, which positions the noise generating sources along the exhaust flow [5]. Each point source is used to predict the broadband noise that the exhaust generates, the contribution of each source is added to the final sound pressure level for an observer [6]. In this work the predictive models DSM-1 and DSM-2 are used to characterize the acoustic field.

Both methods start with locating the flow axis relative to the vehicle and estimating the overall acoustic power [3]

$$W_{OA} = \frac{\eta}{2} n F U_e, \tag{1}$$

where W_{OA} is the overall acoustic power in watt [W], F is the thrust of each engine in newton [N], U_e is the nozzle exit velocity in metres per second [m/s] and η is the acoustical efficiency and n is the number of engines. The acoustical efficiency is usually between 0.2% and 1%. This parameter was deduced [7] from a set of assumptions on the aerodynamic flow characteristics, which provided a mean value around 0.53% [8, 2, 9], a value used on the simulations of this work.

The overall sound power level, L_W, is given by

$$L_W = 10 \log \left(\frac{W_{OA}}{10^{-12}\mathrm{W}} \right), \tag{2}$$

where 10^{-12}W is the reference power.

In case the space vehicle has more than 1 engine, the equivalent nozzle-exit diameter d_e is estimated from $d_e = \sqrt{n} d_{ei}$, where the d_{ei} is the exit diameter of each nozzle.

After determining these parameters, one must start allocating the sources along the flow, and the techniques for each method will be described below.

The DSM-1 method allocates the sound sources along the exhaust flow through empirical curves, each source represents a frequency band in an octave or 1/3 octave bandwidth. This technique is estimated to have an accuracy of ± 4 dB when exhaust shielding and reflections are of little importance [3].

For the allocation of the sources the figure (1) is used, where the solid line curve is the preferred one [3]. Each source represents the centre of each frequency band. With the Strouhal number of each band centre, the respective apparent source axial position is found in terms of the equivalent nozzle exit diameter.

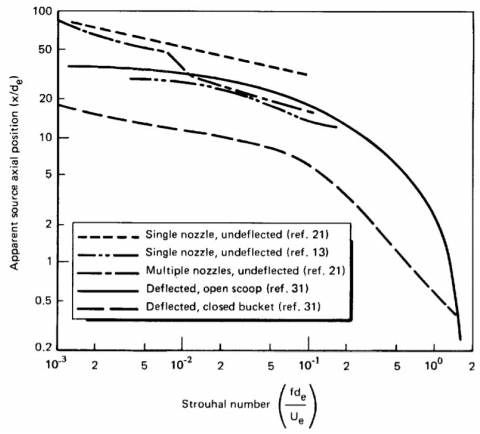

Figure 1: Axial location of apparent sources as a function of Strouhal number [3].

In DSM-2 each source has the entire frequency spectrum, the noise in each frequency band is generated along the flow. A more complex method but more realistic approach when considering the complex nature of the rocket exhaust [6].

The method introduces a new parameter, the core length of the flow, used to distribute the sound power along the flow [2]. The source distribution is made through the division of the flow into slices, where at the center of each slice, a source lies. This is represented in the figure (3).

The length of the core is a parameter only used in the DSM-2, which is dependant on the exit diameter d_e and exit Mach number M_e. It can be determined through

$$x_t = 3.45 d_e (1 + 0.38 M_e)^2. \quad (3)$$

This equation results from a fit to rocket experimental data [3]. Due to its empirical nature other equations have been suggested, discussed in the next section.

The number of slices in the flow division is up to the user, with a value of 20 slices or 200 slices having negligible difference.

Given the allocation of sources along the core length, each source is associated with a power according to its distance to the nozzle as seen in figure (2).

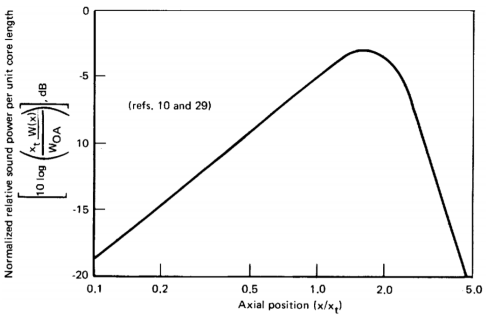

Figure 2: Source power distribution [3].

This method is the more fully featured of the two methods [10] and the most realistic, hence why it is the most studied. Although the methods were published in 1971, it is still considered as the most widely used empirical procedure to predict noise generation of rockets [6].

The next step in both methods is to determine the sound-pressure level SPL_p, and at any point p on the vehicle from:

$$SPL_{b,p} = L_{W,b} - 10 \log r^2 - 11 + DI(b, \theta), \quad (4)$$

where r is the length of the radius line from the source to the observer, θ is the angle between the flow centreline and r and $DI(b, \theta)$ is the directivity at the angle θ for the band centered on the frequency b. For a better representation, see figure (3). In equation (4) new parameters can be added to take into account effects such as reflections and atmospheric absorption, and the latter is calculated in this work, and is given by equations (1) in [11] and (1,4,5,6) in [12].

The directivity is an empirical term that has been subject to different modifications. These models will be presented in the section 3.

The overall sound pressure level at point p ($OASPL_p$) is calculated by adding the SPL in each frequency for the DSM-1 method, but in the DSM-2 method the SPL for each frequency for each slice need to be added, which gives the following equation,

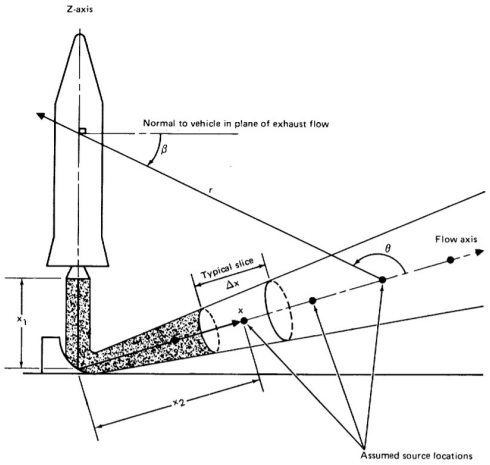

Figure 3: Geometry for the sources and an observer at the suface of the rocket [3].

$$OASPL_p = 10 \log \sum_{Allb} \left[10^{\frac{SPL_{b,p}}{10}} \right]. \tag{5}$$

2.2. Trajectory Determination

This work does not aim at determining the rocket trajectory up to orbit, only the initial stages of flight, thus only considering the vertical ascent and gravity turn for the rocket's first stage. Considering a uniform gravitational force field, the sum of the forces on the axial and transverse direction satisfy, respectively, the equations [13]

$$\frac{dX}{dt} = V \cos\gamma, \tag{6}$$

$$\frac{dH}{dt} = V \sin\gamma, \tag{7}$$

$$m\frac{dV}{dt} = T - D - \left(mg - \frac{m\dot{X}^2}{R+H} \right) \sin\gamma, \tag{8}$$

$$mV\frac{d\gamma}{dt} = -\left(mg - \frac{m\dot{X}^2}{R+H} \right) \cos\gamma, \tag{9}$$

where R is the radius of the Earth, X is the downrange and γ the vehicle flight path angle.

D is the drag law, and is defined as

$$D = \frac{1}{2} C_D A \rho V^2, \tag{10}$$

where ρ is the atmospheric density, V is velocity of the rocket, A is the frontal area of the booster and C_D the drag coefficient.

The vertical ascent is set by applying $\gamma = 90°$and the gravity turn with a $d\gamma/dt \neq 0$.

For the gravity turn, the force of gravity is modified to include the apparent centrifugal force [13]. The gravity turn equations of motion have no analytical solution, and in this work the 4th Order Runge-Kutta method was used to integrate the equations.

3. Model Improvements

3.1. Sound Directivity Models

The sound pressure level of the exhaust flow does not propagate spherically, thus the introduction of directivity, a term to account for the sound pressure contour [14]. This parameter varies from engine to engine [6], but the models use an empirical adjustment to far-field measurements, nonetheless useful in near-field acoustic predicitons [3].

Eldred [3] presented a set of curves derived from a set of experimental data from different rocket engines. The directivity index is a frequency dependant term, varying according to the angle between the flow axis and the observer. A set of equations to fit the empirical curves were suggested at [6], corrected at [15] and are given by the following equations,

- if $\theta < 23 + 12\mathrm{St}^*$

$$DI(St,\theta) = (0.4{-}0.07St^*)(\theta{-}35{-}8St^*){+}13{-}2.6St^*$$

- if $23 + 12\mathrm{St}^* < \theta < 90 + 12\mathrm{St}^*$

$$DI(St,\theta) = (0.035St^*{-}0.28)(\theta{-}35{-}10St^*){+}6.5{-}St^*$$

- if $\theta > 90 + 12\mathrm{St}^*$

$$DI(St,\theta) = -0.1\theta - 0.3 + 2St^*$$

Where St^* is a modified Strouhal number, defined as

$$St^* = \log_{10}\left(\frac{f d_e}{U_e}\right) + 3,$$

The comparison between the fit and the empirical curves are presented in figure 4.

Another model for undeflected flow was proposed by Sutherland and Plotkin [4]. The model combines theoretical and experimental works done previously [6]. The expression proposed is given below

$$\begin{aligned} DI(St,\theta) =& 10\log_{10}\left[\frac{C_1\left[1 + (\cos(\theta_e))^4\right]}{\left[(1 - M_{ec}\cos(\theta_e))^2 + 0.3M_{ec}^2\right]^{2.5}\left[1 + C_2\exp\left(-C_3\theta_e\right)\right]} \right] + \Delta \\ \Delta =& -C_4\log_{10}(St) - C_5. \end{aligned} \tag{11}$$

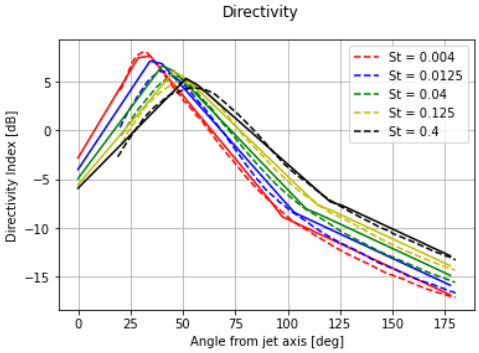

Figure 4: Eldred directivity curves in dashed lines and the correspondent results from the fit equations in full lines [3].

The C constants are given as $C_1 = 0.37$, $C_2 = 310$, $C_3 = 9$, $C_4 = 0.698$, $C_5 = 1.67$ and $M_{ec} = 0.75$ is the typical eddy convection Mach number for a heated jet. The parameter θ_e is given by

$$\theta_e = \theta - 9.61 \log_{10} \left[\frac{St}{DI_{max}} \right], \qquad (12)$$

where DI_{max} is the maximum directivity index, set equal to 0.0515 and θ_e is the angle between the flow axis and the observer.

In the figure (5), is represented the directivity index for different Strouhal numbers at a wide range of angles. The data follows in general the plots from Eldred [3], although from 90 to 140 degrees, the directivity index is lower than what suggested the Eldred empirical curves.

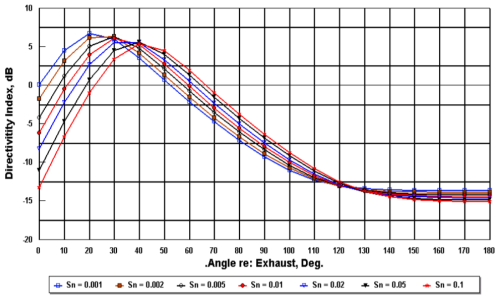

Figure 5: Directivity Index according to Sutherland and Plotkin [4].

Other set of empirical curves were suggested [14], which were obtained during a series of tests on three RSRM (Reusable Solid Rocket Motor, used for the Space Shuttle) for far-field acoustic measurements. The curves were later modified to account for the apparent axial source location for each frequency [16]. The results are presented in the figure (6)

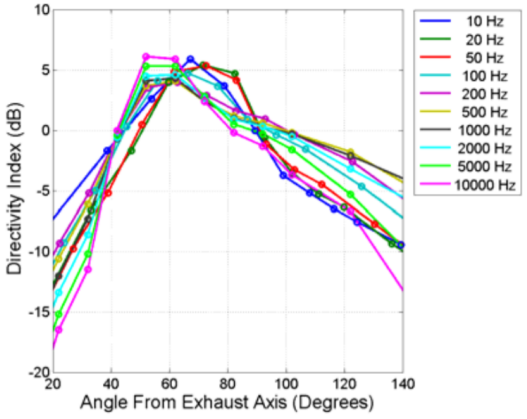

Figure 6: Modified RSRM Directivity Index [16].

3.2. Laminar Core Length Models

The DSM-2 uses the parameter laminar core length to distribute the sound pressure along the exhaust flow, as mentioned before. An empirical model for the laminar core length x_t was presented by Eldred [3], and is given by equation (3).

A set of static tests, according to Varnier [2], showed that the Eldred laminar core length model did not predict the sound pressure in near-field appropriately and needed a correction. The study then suggested a new model, given by

$$x_t = 1.75 D_e (1 + 0.38 M_e)^2. \qquad (13)$$

A recent study, through experimental data as well, proposed an alternative model. The model is a result from a comparison of both models above, it stroke a balance between the two, this led to the following equation

$$x_t = 2.875 D_e (1 + 0.38 M_e)^2. \qquad (14)$$

3.3. Model Analysis as function of Experimental Data

A set of simulations were done to compare the models to experimental data in order discuss for both DSM-1 and DSM-2 which models better fit the experimental data. The DSM-2 will be divided into 2, an analysis on the core length models and on the directivity models, and the DSM-1 only the directivity models. Important to note that the Haynes directivity model is harder to use due to its limited angle span, not providing values above 140°and below 20°. One can use a linear fit to extend for the smaller angles, but for angles above 140°is much more difficult to pinpoint with small margins of error the directivity index. As such, a priori the Eldred and Plotkin directivity are preferred to Haynes's directivity model.

The figures (7),(8),(9) and (10) represent the OASPL as function of x/D_e obtained in this work

and the experimental data at [10]. Each graph represents a different model, the green "x" represent the experimental data and the black dots represent the James et al. data at the same x/d_e as the experimental data. In table (1) are the directivity models that best represents each test.

Analyzing overall the results, the DSM-2 Varnier model is best represented by the Plotkin directivity model although closer to the nozzle exit the values are underpredicted in all cases. The Plotkin directivity is underpredicting in most points and the results for Eldred directivity are very close to Plotkin's, but overpredicting the experimental data, which is a strong argument to avoid poorly estimating the impact in the communities.

DSM-2 Eldred core length model is best represented by Haynes, although underpredicting in all points for all cases. The Varnier core length model best fits the experimental data. The DSM-2 method has the best results using the Varnier core length model with Eldred directivity model.

Overall Eldred directivity is the best fit for DSM-1, but figure (7) has results worst results. As before, Eldred model is overpredicting the OASPL in most points, with results in the proximity of the curve.

Using DSM-2 Varnier core length model and Eldred directivity model provide the best results to estimate the acoustic loads, although for moving sources the acoustic loads are overpredicted across every metric, since the models are for undeflected flow at launch and a decrease is expected when the rocket is in forward flight (moving sources).

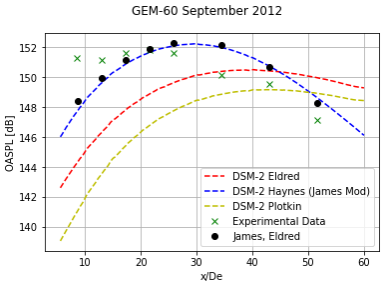

(a) DSM-2 Eldred Core Length.

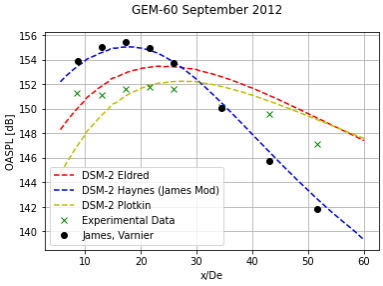

(b) DSM-2 Varnier Core Length.

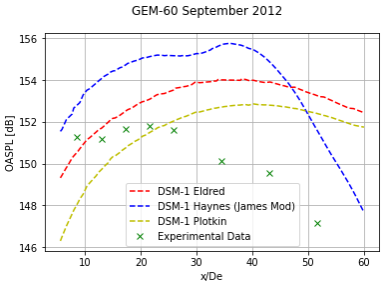

(c) DSM-1.

Figure 7: Comparison of results from this Work and James et al. (2016) GEM-60 September 2012 experimental data.

4. Results

4.1. Location

The case study chosen is the, still to build as of writing this work, Santa Maria Spaceport due to the interest in understanding the impact it may have on the communities livelihood. To study the problem a set of considerations were applied. The specific launch location has not been disclosed to the public, as of writing this work, which leads to some degree of freedom in choosing the location. Relying only on satellite imagery, the launch site was chosen in the south region (most distant to the villages) with enough ease of access (roads), with favorable launch azimuth (discussed below) and moved away from the cliff to minimize reflections and echo. The launch point is coincident with the rockets position in figure (11 a)

The locations that were chosen for a more detailed study were the most populated village and the nearest to the launch site, the Vila do Porto and Santo Espirito respectively.

The size of Santa Maria island restricts the rockets that can be launched due to the maximum distance between the regions. In this work, the Falcon 9 rocket was chosen as an upper bound of the largest rocket possible to launch in Santa Maria, since its highly reliable [17].

The initial idea for the construction of the spaceport was to launch nanosatellites into orbit, which can be done with microlaunchers. A very well studied rocket is the Electron, the representing the typical rocket in this work that could be launched at the Santa Maria spaceport.

To diminish the noise event duration, the rocket should not overfly the island. There is a preference for an eastern launch due to Earth's rotation. With these two conditions, the limits of the azimuth are 95°to 180°.

4.2. Falcon 9 Results

The necessary rocket parameters used as input for the simulations are present in a acoustic experiment study [18]. The simulations were performed by calculating the contours in a plane at the same level as the launch point, assuming a terrain with no ir-

Table 1: Best fit for the Experimental data [6]

	GEM-60 Sep 2012	GEM-60 Feb 2009	Orion 50S XLG	GEM-60 Jun 2008
DSM-2 Varnier CL.	Plotkin	Plotkin	Eldred/Plotkin	Eldred
DSM-2 Eldred CL.	Haynes	Haynes	Haynes	Haynes
DSM-2 CL. Models	Varnier	Varnier	Varnier	Varnier
DSM-1	NONE	Plotkin	Eldred	Eldred

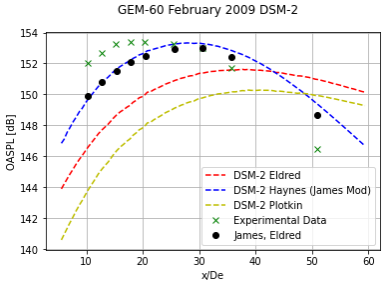

(a) DSM-2 Eldred Core Length.

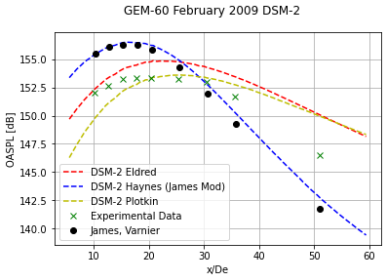

(b) DSM-2 Varnier Core Length.

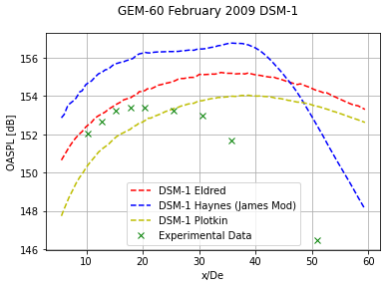

(c) DSM-1.

Figure 8: Comparison of results from this Work and James et al. (2016) GEM-60 February 2009 experimental data.

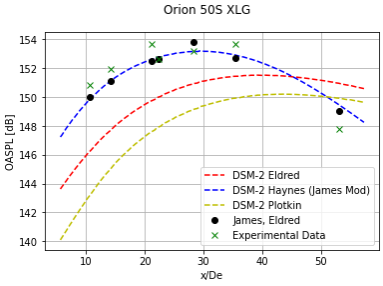

(a) DSM-2 Eldred Core Length.

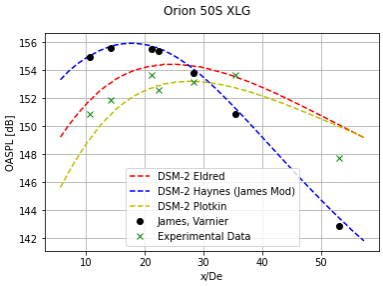

(b) DSM-2 Varnier Core Length.

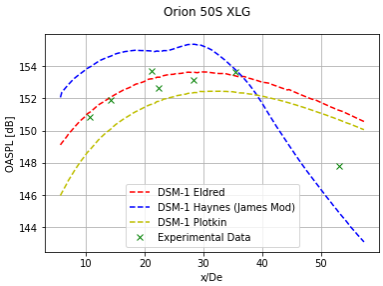

(c) DSM-1.

Figure 9: Comparison of results from this Work and James et al. (2016) Orion 50S XLG experimental data.

regularity and no reflections. This assumption is a limitation of this work since at West of the launch site one can find a valley, source of reflections and echo. The trajectory used to compute said simulations, replicates that of [18].

In figure (11) and (12), are represented different stages of the flight with different contour shapes with their respective magnitude in between each line, and the black dot represents the position of the rocket. The axis in the figure represent the distance, in meters, to the launch point (origin of the axis) and to the right of the figures (a) to (c), 4 rocket parameters are displayed. In the figure (11) the rocket launch azimuth is 180°, whereas at the figure (12) the rocket launch azimuth is 95°. The first two stages in figure (11) are not influenced by the launch azimuth, as such it is expected that the 95°launch azimuth has the same contours as 180°for (a) and (b).

To get a better grasp of the acoustic levels across time in the Vila do Porto village and on the closest village, Santo Espírito, the figures (13) and (14)

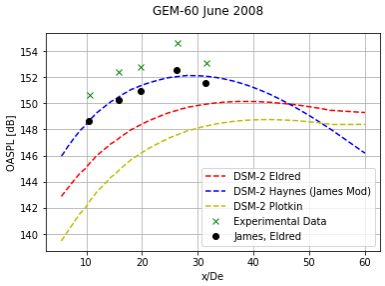

(a) DSM-2 Eldred Core Length.

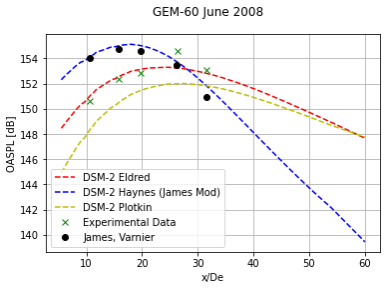

(b) DSM-2 Varnier Core Length.

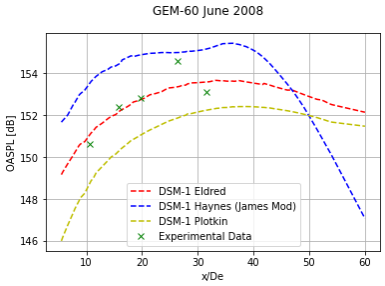

(c) DSM-1.

Figure 10: Comparison of results from this Work and James et al. (2016) GEM-60 June 2008 experimental data.

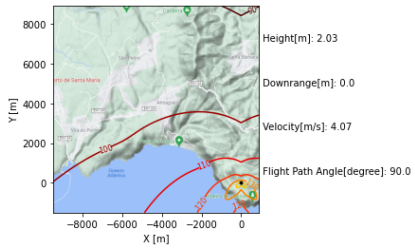

(a) Beginning of Launch

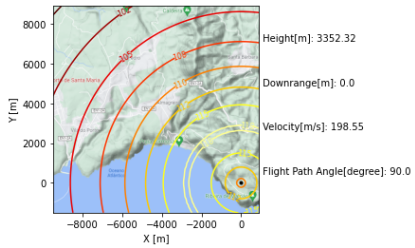

(b) Without deflector influence

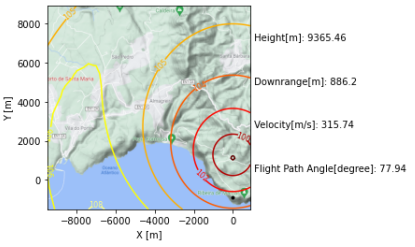

(c) Pitchover Maneuver

Figure 11: OASPL Contours for Falcon 9 rocket using a 180°Launch Azimuth.

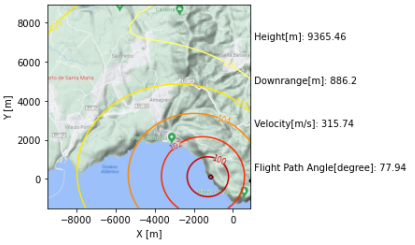

(a) Pitchover Maneuver

Figure 12: OASPL Contours for Falcon 9 rocket using a 95°Launch Azimuth.

were computed

Vila do Porto has a maximum OASPL of 110.3 dB and a maximum A-weighted OASPL of 90.1 dBA. The Sound Exposure Level is computed (SEL) using the 10-dB down time, resulting in an SEL of 105.09 dB for the 95°launch azimuth, while the 180°launch azimuth presents an SEL of 105.25 dB. Comparing the launch azimuths, its seen that the 95°launch azimuth presents lower acoustic levels for the Vila do Porto village but the SEL presents a minor decrease, suggesting that overall both trajectories do not separate much from each other.

The Santo Espírito village is the most affected due to its closeness to the point of launch, with a maximum OASPL of 116.9 dB and A-weighted of 99.4 dBA as seen in figure (14). The SEL in the Santo Espírito village for the 95°launch azimuth is 113.90 dB and for the 180°launch azimuth an SEL of 113.59 dB. In this case the better launch azimuth is the 180°, contrary to what was seen before. Thus it is not clear as to which trajectory is better overall, concluding that as for the noise there is no need for maneuvers to minimize the noise.

The Occupational Safety and Health Standards (OSHA) recommends a A-weighted OASPL maximum of 115 dBA for a duration of 0.25 hours or less [19] for hearing conservation, and since the noise events last less than a few minutes this value will be considered. The World Health Organization (WHO) recommended a maximum A-weighted OASPL of 110 dBA to avoid acute damage to the

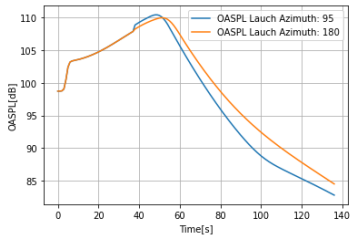

(a) Vila do Porto Falcon 9 OASPL

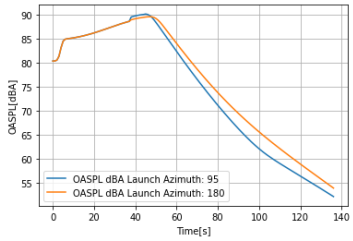

(b) Vila do Porto Falcon 9 A-Weighted OASPL

Figure 13: Vila do Porto Falcon 9 Noise Metrics.

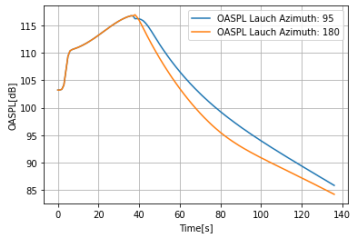

(a) Santo Espírito Falcon 9 OASPL

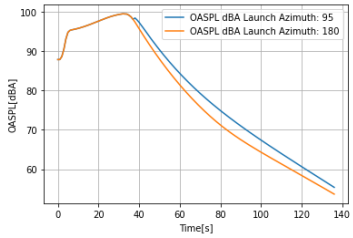

(b) Santo Espírito Falcon 9 A-Weighted OASPL

Figure 14: Santo Espírito Falcon 9 Noise Metrics.

human inner ear [20]. Its seen that for the Falcon 9 none of the trajectories exceed the threshold, and even considering the error of ±4dB from the numerical models the upper limit is still below the threshold.

According to OSHA, for structural damage it is used the maximum OASPL, where for 1 in 100 households exposed to 120 dB will claim damage and 1 in 1000 will claim damage when exposed to 111 dB [19] and according to the WHO in order to avoid and minimise the risk of structural damage an OASPL of 110 dB should not be exceeded. Taking into account the ±4 dB error, the Vila do Porto having a max OASPL of 110.3 dB would exceed the WHO and the OSHA 111 dB threshold, and the Santo Espirito exceeds all of the above.

Based on these results, the Falcon 9 can not launch on the Santa Maria Island without recurrent collateral damage on the structures. Having metrics close to the threshold implies the need for more detailed and accurate results to evaluate the potential of launching in the Santa Maria spaceport.

4.3. Electron Results

To compute the contours, the trajectory was computed by considering a gravity turn starting at time set at 20s and an initial pitch angle of 88°. Using the same conditions as the Falcon 9 results section the OASPL contours are given in the figure (16) and (15) for the 95°and 180°launch azimuths respectively.

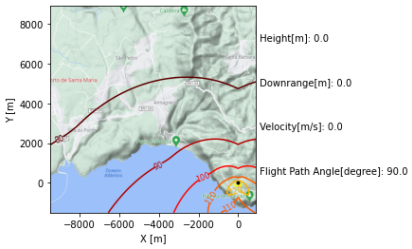

(a) Beginning of Launch

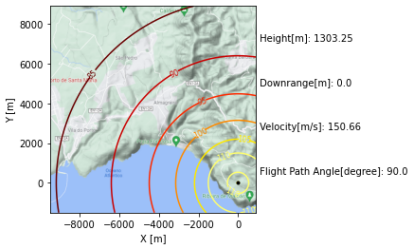

(b) Without deflector influence

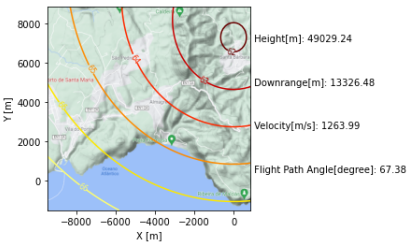

(c) Pitchover Maneuver

Figure 15: OASPL Contours for the Electron rocket using a 180°Launch Azimuth.

The OASPL contours are very similar to those on figures (12) and (11), with the differences being on the magnitude of the OASPL and on the Pitchover maneuver figure where the rocket is at a height of 50 km, where one can observe the directivity in the later stages of the considered trajectory.

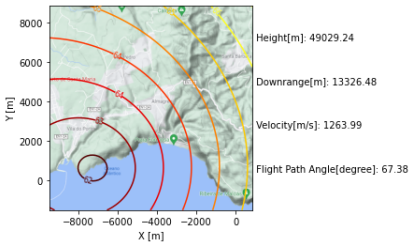

(a) Pitchover Maneuver

Figure 16: OASPL Contours for the Electron rocket using a 95°Launch Azimuth.

To ascertain the effects on the communities separate noise metrics were computed to follow the acoustic loads on the villages. For the Vila Porto and Santo Espírito villages, the graphs are presented in the figures (17) and (18) respectively.

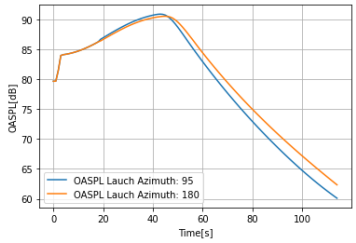

(a) Vila do Porto Electron OASPL

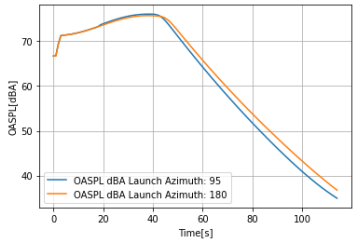

(b) Vila do Porto Electron A-Weighted OASPL

Figure 17: Vila do Porto Electron Noise Metrics.

The Vila do Porto village has an SEL of 91.28 dB for the 95°launch azimuth and an SEL of 91.30 dB for the 180°launch azimuth. The maximum OASPL and A-weighted OASPL are 91 dB and 76 dBA, respectively. The Santo Espírito has an SEL of has an SEL of 101.24 dB for the 95°launch azimuth and an SEL of 101.19 dB for the 180°launch azimuth. The maximum OASPL and A-weighted OASPL are reached at time 30s with the respective values of 99 dB and 87.5 dBA.

Given the hearing conservation threshold by OSHA and WHO, the values of max A-weighted are below the 115dBA and 110dBA mark respectively. As for the structural damage threshold given by the same entities, both villages are below the suggested OASPL. With these results it is possible to approve

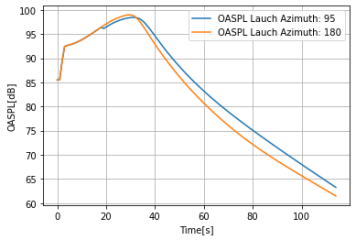

(a) Santo Espírito Electron OASPL

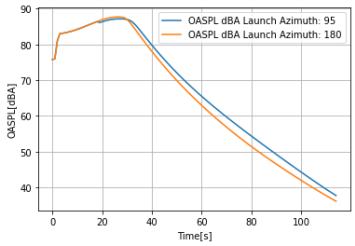

(b) Santo Espírito Electron A-Weighted OASPL

Figure 18: Santo Espírito Electron Noise Metrics.

the launch of rockets in the same category as Electron, since the acoustic levels are significantly below the threshold mark.

5. Conclusions

In this work the main objective was to predict noise from launching rockets at the early stages of flight and compute the noise metrics, which is then applied to the Santa Maria spaceport. This is achieved by developing a tool capable of computing noise contours and initial trajectory of rockets.

The prediction of noise was done using the semi-empirical methods DSM-1 and DSM-2, which have been subject to various modifications due to the limitations and shortcomings of the models. The modifications discussed in this work were acoustic efficiency, directivity and laminar core lengths models, which are then compared to determine the best fits to the goal of this work. The acoustic efficiency was chosen based on the literature, meanwhile the remaining two were based on the literature and on comparisons with experimental data.

The simulations in the Santa Maria spaceport were performed for the Falcon 9 and Electron rockets, using the 180°and 95°launch azimuths. The OASPL and A-weighted OASPL were computed for the regions of Santo Espírto and Vila do Porto, chosen based on the proximity and population respectively. The Electron rocket results do not break any of the guidelines by OSHA and WHO, with enough room for a more potent rocket. The Falcon 9 had inconclusive results since the metrics were close to the stipulated threshold, thus needing a more accurate experiment or simulation to determine its launch viability in Santa Maria.

References

[1] Jacky Huart. Space-innovation ecosystem in santa maria. /https://ptspace.pt/space-innovation-hub-santa-maria/, 2016. Retrieved: 2020-11-10.

[2] Jean Varnier. Experimental study and simulation of rocket engine freejet noise. *AIAA Journal*, 39(10):1851–1859, 2001.

[3] K.M Eldred. Acoustic loads generated by the propulsion system. *NASA Technical Note SP-8072*, 1971.

[4] Kenneth Plotkin, Louis Sutherland, and Bruce Vu. Lift-off acoustics predictions for the ares i launch pad. *15th AIAA/CEAS Aeroacoustics Conference (30th AIAA Aeroacoustics Conference)*, 2009.

[5] Linamaria Perez and Daniel C Allgood. Prediction of acoustic loads generated by propulsion systems. *NASA USRP – Internship Final Report*, 2011.

[6] Wesley Oliver Smith III. *An Empirical and Computational Investigation into the Acoustical Environment at the Launch of a Space Vehicle*. PhD thesis, Auburn University, December 2013.

[7] Louis Sutherland. Progress and problems in rocket noise prediction for ground facilities. *15th Aeroacoustics Conference*, 1993.

[8] Damiano Casalino, Mattia Barbarino, Mariano Genito, and Valerio Ferrara. *Improved Empirical Methods for Rocket Noise Prediction Through CAA Computation of Elementary Source Fields*.

[9] Damiano Casalino, Mattia Barbarino, Mariano Genito, and Valerio Ferrara. Hybrid empirical/computational aeroacoustics methodology for rocket noise modeling. *AIAA Journal*, 47(6):1445–1460, 2009.

[10] Michael M. James, Alexandria R. Salton, Kent L. Gee, and Tracianne B. Neilsen. Comparative analysis of nasa sp-8072's core length with full-scale rocket data. *Transactions of the Japan Society for Aeronautical and Space Sciences, Aerospace Technology Japan*, 14, 2016.

[11] H. E. Bass, L. C. Sutherland, and A. J. Zuckerwar. Atmospheric absorption of sound: Update. *The Journal of the Acoustical Society of America*, 88(4):2019–2021, 1990.

[12] H. E. Bass, L. C. Sutherland, A. J. Zuckerwar, D. T. Blackstock, and D. M. Hester. Atmospheric absorption of sound: Further developments. *The Journal of the Acoustical Society of America*, 97(1):680–683, 1995.

[13] William E Wiesel. *Spaceflight dynamics*. Aphelion Press, 3rd edition, 2010.

[14] Jared Haynes and Robert Kenny. *Modifications to the NASA SP-8072 Distributed Source Method II for Ares I Lift-Off Environment Predictions*. 2009.

[15] Fredrik Ranow. Acoustic prediction methods for rocket flame deflector design. Master's thesis, KTH, School of Industrial Engineering and Management (ITM), 2021.

[16] Michael M. James, Alexandria R. Salton, Kent L. Gee, Tracianne B. Neilsen, Sally A. McInerny, and R. Jeremy Kenny. Modification of directivity curves for a rocket noise model. *Proceedings of Meetings on Acoustics*, 18(1):040008, 2012.

[17] Ed Kyle. Space launch report. /https://www.spacelaunchreport.com/log2020.html#rate. Retrieved: 2021-10-20.

[18] Logan T. Mathews, Kent L. Gee, and Grant W. Hart. Characterization of falcon 9 launch vehicle noise from far-field measurements. *The Journal of the Acoustical Society of America*, 150(1):620–633, 2021.

[19] Federal Aviation Administration. *Draft Programmatic Environmental Assessment for the SpaceX Starship/Super Heavy Launch Vehicle Program at the SpaceX Boca Chica Launch Site in Cameron County, Texas*, 2021. /https://www.faa.gov/space/stakeholder_engagement/spacex_starship/media/Draft_PEA_for_SpaceX_Starship_Super_Heavy_at_Boca_Chica.pdf, Retrieved: 2021-10-26.

[20] United Kingdom Department of Transport. *Draft Guidance to the regulator on environmental objectives relating to the exercise of its functions under the Space Industry Act 2018*, 2021. /https://assets.publishing.service.gov.uk/government/uploads/system/uploads/attachment_data/file/958464/draft-guidance-to-the-spaceflight-regulator-on-environmental-objectives.pdf, Retrieved: 2021-10-25.